A Study of Material and Architectural Effects on the Impact Response of 2D and 3D Dry Textile Composites using LS-DYNA®

Gaurav Nilakantan [a,b], Michael Keefe [a,d], John W. Gillespie Jr. [a,b,c,*]
Travis A. Bogetti [e], Rob Adkinson [e]

[a] Center for Composite Materials
[b] Department of Materials Science and Engineering
[c] Department of Civil and Environmental Engineering
[d] Department of Mechanical Engineering
University of Delaware, DE 19716, USA

[e] US Army Research Laboratory
Aberdeen Proving Ground, MD 21005, USA

Abstract

High strength 2D fabrics and 3D textile composites comprised of materials such as Kevlar™, Vectran™, Zylon™, and S2-Glass® find applications in protective systems such as personnel armor, spall liners, and turbine fragment containment. Various parameters can significantly affect the response of these fabrics under high rate impact including yarn/tow geometry (cross section), yarn/tow material (modulus, strength), and architecture (undulations and span). However these are just a few of the many other parameters such as projectile characteristics, boundary conditions, number of layers and orientations, weaving degradations, and so forth. Many of these parameters are inter-related and unfortunately this makes a comprehensive study very complex. Therefore, a set of key parameters have been identified for an initial exploratory numerical investigation. These include, on the material front: yarn/tow axial modulus, strength, frictional coefficient; and on the architectural front: yarn/tow cross section shape, size, span, and angle of inclination of through-thickness stitching or Z-tows. This study provides interesting initial insight into the role of through thickness tows on the overall impact resistance and energy dissipation capabilities for which these high strength fabrics were designed for. 3D fabrics with varying Z-tow architectures are compared against each other as well as against 2D fabrics without through thickness stitching. A special in-house preprocessor DYNAFAB is used to automatically generate the entire textile composite mesh. The user inputs basic parameters describing the desired yarn/tow geometry, architecture, and mesh density. The output is a LS-DYNA keyword input-file ready to use in the simulation. The geometry and undulations in the FE model closely represents the actual micrographs of the textile composite leading to a realistic representation of the architecture.

Keywords: plain weave fabric, 3D textile composite, architectural and material effect, transverse impact, finite element analysis, LS-DYNA, preprocessor, DYNAFAB

[*]Corresponding author. Tel.: +1(302)831-8149, *Email address*: gillespi@udel.edu
John W. Gillespie Jr.
Director, Center for Composite Materials

1. INTRODUCTION

2D and 3D fabrics respectively comprised of high strength continuous filament yarns or tows are used in protective structural applications that require penetration resistance against incident high energy projectiles. Typical examples of high strength materials used are Kevlar, Twaron, Vectran, and S2-glass. Applications include body armor, spall liners, turbine fragment containment, ceramic tile backing, and structural reinforcements. 3D fabrics have a few distinct benefits over 2D fabrics in impact performance. Most notable is that the 3D fabric warp and fill tows do not have any crimp unlike in 2D fabric warp and fill yarns. Three attributes detrimental to impact performance associated with increased amounts of crimp are (i) longer time for yarns to decrimp before they develop tension through elongation (ii) lesser packing ability or lower areal density, and (iii) greater weaving damages. When comparing 2D plain weave and 3D fabrics, these properties will generally have the following effects. The first attribute implies the 3D fabric will initially decelerate the projectile faster that a 2D fabric. The second attribute implies a greater extent of initial momentum transfer between the projectile and fabric. The third attribute implies the strength retention of warp and fill tows in 3D fabrics without tow crimp will be higher than warp and fill yarns comprised of the same material in plain weave fabrics. However 2D fabrics such as the plain weave architecture also possess two distinct advantages when used in personnel protective clothing. This first is that before the locking angle is reached, they are flexible and shearable which is important since the fabric needs to adjust to the contours of the human torso and extremities so that the protective clothing can be worn comfortably. In a 3D fabric the Z-tows play a vital role in holding all the warp and fill tow layers together. Without Z-tows, a small projectile could simply push aside the warp and fill tows with little resistance. In a 2D fabric, the through thickness stitching yarns serve the purpose of holding the various layers together. However because the warp yarns are woven with the fill yarns, the stitching yarns are not vital to the 2D fabric. This is the second advantage of the 2D fabrics. Thus a detailed study of the material and architectural effects is required in order to make the best judgment as to which combination of geometry and material properties would yield optimal impact performance.

In our recent work [1], we had begun an investigation into the effect of 3D architecture on the impact response of flexible fabrics. Here 'flexible' refers to dry fabrics without any resin impregnation. 2D plain weave fabrics were compared to 3D fabrics. The generic 3D fabric architecture selected for the study was similar to that of the 100 oz 3WEAVE^{TM} S2 fabric from 3TEX, Inc. Dimensions obtained from micrographs were used as input while creating the fabric mesh such that all tow cross sections and undulations were realistically modeled. Then a generic 2D plain weave fabric was modeled such that it was geometrically and materially equivalent to the 3D fabric in terms of number of yarns, yarn spans, fabric thickness, areal density, and yarn material properties. This allowed a direct qualitative and quantitative comparison of impact performance. It was observed from this study that 3D fabrics outperformed 2D fabrics for both non-penetrating and penetrating impact cases in terms of dynamic deflections, time taken to arrest the projectile or residual projectile velocity, and energy absorptions. Further, varying the angle of inclination of the Z-tows from the original value of 67.7° to 90.0° increased the impact performance. The improvement was explained by the greater 'crimp' because of the longer path length of the Z-tows in the latter case exerting lesser deformations and stresses on the corresponding interlaced fill tows, leading to the delayed boundary failure of a fewer number of fill tows present at the impact location. Thus before the first failure of the fill tows around the impact region, both 3D fabric architectures yielded similar performance. However after the first failure of the fill tows in the 67.7° case, the impact performance improvement was observed for the 90.0° case. In another part of the same study [1], three layers of 2D plain weave fabrics both with and without stitching yarns were compared with each other for penetrating impact velocities. The effect of the stitching yarns greatly improved the performance. Interestingly, the improvement was not due to the extra elastic strain energy absorbed by the stitching yarns, rather it was that the stitching yarns kept the top most or impacted layer engaged with the rest of the fabric during the projectile penetration, thereby increasing the total elastic strain energy which directly contributed to slowing down the projectile. For the 2D fabric case without the stitching yarns, after the impacted yarns in the top most layer failed, the layer simply separated from the rest of the fabric and flapped freely, no longer contributing to slowing down the projectile. Thus it was concluded that a 3D architecture, in terms of the 3D fabric, and 2D fabric with stitching yarns, significantly contributed to impact performance.

In this study, the previous statement is further explored by first considering material effects of the fill and Z-tows used in our previous work [1]. Next, multiple plies of the earlier studied 2D and 3D fabrics for both non-penetrating and penetrating cases are investigated using projectiles of different shapes

but having the same initial momentum. By understanding the role of architecture and material on the impact performance of 2D and 3D fabrics through the various deformation, energy absorption, and interaction mechanisms, superior protective structures can be designed.

2. SETUP OF THE FABRIC FINITE ELEMENT MODELS

The setup of the fabric finite element (FE) models used in Ref. [1] has been repeated here for the convenience of the reader, also the new models used in this study are described in this section.

2.1 SETUP OF THE 2D PLAIN WEAVE FABRIC

Figure (1) displays a micrograph of a generic plain weave fabric showing the undulations and cross section of the warp and fill yarns respectively. The geometrical parameters with respect to Figure (1) are assumed as follows: (s) 3.0 mm (w) 2.2 mm (t) 0.458 mm. It is assumed that both warp and fill yarns have the same cross section and undulations. As will be seen later, the geometrical parameters were so chosen so as to enable a direct comparison with the 3D fabric architecture used in this study.
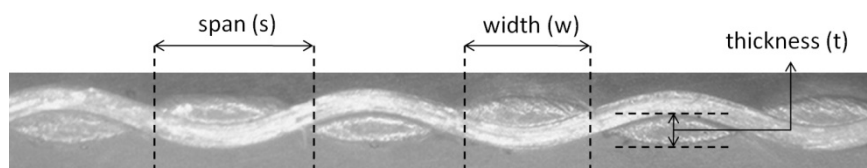

Figure 1. Micrograph of a generic 2D plain weave fabric

Figure 2. Corresponding FE model

Figure (2) displays the corresponding FE model of the micrograph shown in Figure (1). The undulations of the warp (fill) yarn control the fill (warp) yarn cross section. The 2D fabric case considered consists of multiple layers of a plain weave fabric. With three layers, it becomes equivalent in thickness to one layer of the 3D fabric, while with six layers it become equivalent in thickness to two layers of the 3D fabric, as shown later. The in-plane dimensions of the fabric are 101.6 mm x 50.8 mm. The total fabric thickness is 2.748 mm for three layers. Figure (3) displays the FE models of the fabric with yarn level architecture meshed using only solid elements (2D-Case #1). Because of symmetry, only one quarter of the FE mesh needs to be modeled.
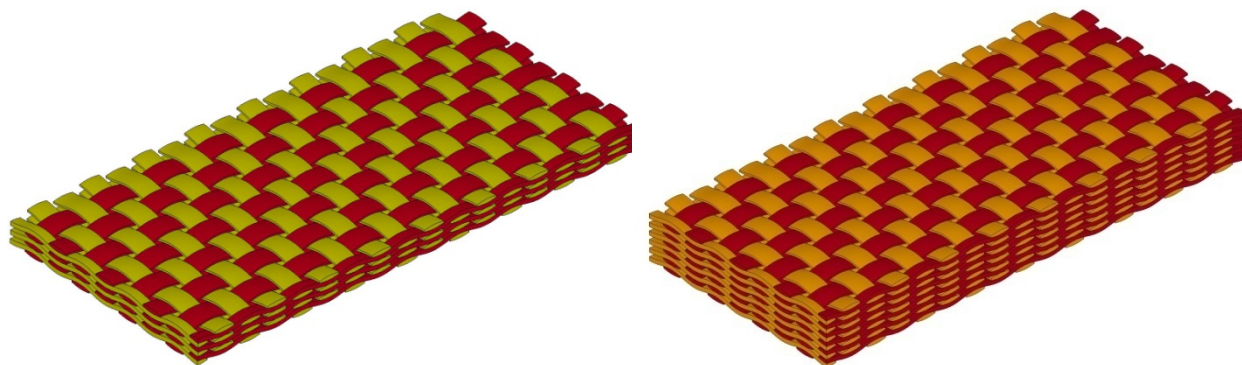

Figure 3. FE model of the 2D plain weave fabric (2D-Case #1) (left) three layers (right) six layers

The orthotropic material properties of the 2D fabric yarns are assigned as follows: Longitudinal modulus (E_{11}) of 80 GPa, Density (ρ) of 3.56 g/cm^3. This density was chosen so that the areal density of this 2D fabric matches that of the 3D fabric described in a later section. Yarn failure via element

erosion is incorporated in LS-DYNA using a maximum principal stress failure criterion (σ_{fail}) of 3.5 GPa. Dry yarns have very little initial resistance to transverse compression or shear because of the filament level architecture, wherein individual filaments simply redistribute themselves under load. For this reason, the transverse elastic moduli (E_{22} and E_{33}) and shear moduli (G_{12}, G_{23}, and G_{31}) are assumed to be one-tenth the longitudinal elastic modulus. This is also a reasonable assumption when modeling a yarn as a homogenized continuum neglecting filament level detail, wherein the predominant material property is the longitudinal modulus. For computational stability reasons, small non-zero Poisson ratios of 0.01 are used.

2.2 SETUP OF THE 3D FABRIC

Figure (4) displays micrographs of one layer the 3D fabric. Dark overlay lines are used to clarify the cross sectional shapes of the warp, fill, and z-tows. The 3D fabric consists of five layers of warp and fill tows that are interlaced with z-tows that run parallel to the warp tows. Figure (4a) displays the undulations of the z-tows along with the cross sectional profiles of the fill tows. As can be seen, the top and bottom fill tows are semi-elliptical in shape while the middle fill tows transition along their length between two trapezium shapes which are vertical mirror images of each other. Figure (4b) displays the cross sectional profiles of the z-tows and warp tows which are rectangular in shape. As can be seen, the tight packing causes the warp tows to be pushed aside by the z-tows. The angle of inclination (θ) of the z-tows with respect to the horizontal is around 67.7°. The dimensions assigned to the tows of the corresponding FE model are as follows - Warp tow: (s) 2.5 mm, (t) 0.55 mm, (w) 2.2mm; Fill tow: (s) 3 mm (t) 0.56 mm; and z-tow (s) 2.5 mm (t) 0.25 mm (w) 1.166, where 's', 't', and 'w' are the span, thickness, and width respectively. The middle layer fill tow with the trapezium cross sectional shape has a longer side of 2.96 mm and a shorter side of 2.5 mm. The upper and lower layer fill tows with the semi-elliptical cross sectional shapes have a semi-major axis of 1.0 mm and a semi-minor maxis of 0.26 mm.
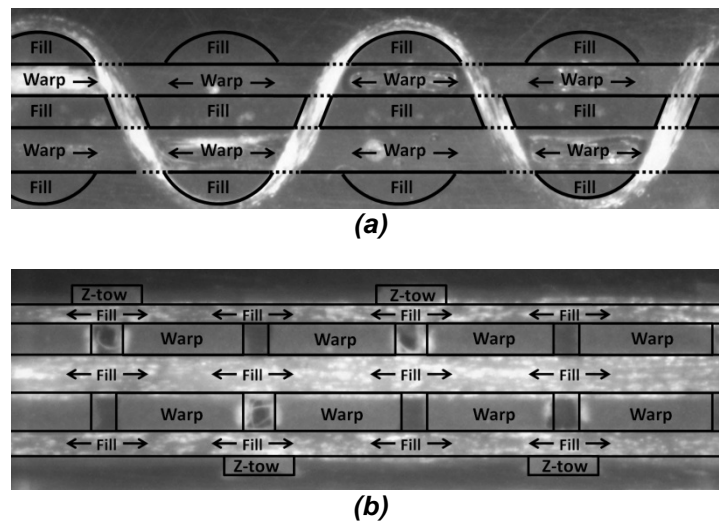

(a)

(b)

Figure 4. Micrographs of the 3D fabric

Figure (5) displays the FE mesh of one layer of the 3D fabric (3D-Case #1) corresponding to the micrographs in Figure (4). Solid elements are used in the mesh to model the tows. The in-plane dimensions of the fabric are also 101.6 mm x 50.8 mm. The total fabric thickness for one layer is around 2.78 mm. The orthotropic material properties of the 3D fabric warp, fill, and z-tows are assigned as follows: Longitudinal modulus (E_{11}) of 80 GPa, Density (ρ) of 2.43 g/cm^3, and a failure stress (σ_{fail}) of 3.5 GPa. Again, the transverse elastic moduli and shear moduli are one-tenth of the longitudinal modulus, and Poisson ratios of 0.01 are used. In order to study the effect of the z-tow inclination, a second 3D fabric case is set up, where the angle of z-tow inclination (θ) is set at 90°. To enable a comparison with the first 3D fabric case, all geometric and material parameters are kept the same with the exception of the upper and lower layer fill tows that now have a wider and thinner semi-elliptical shape as follows: semi-major axis of 1.375 mm and a semi-minor maxis of 0.4072 mm. Figure (6) displays the FE mesh of one layer of the second case of the 3D fabric (3D-Case #2). In the first

part of this study, only one layer of 3D fabrics are used. In the second part of this study, two layers of 3D fabrics are used with one layer stacked over the other layer with perfect alignment. An additional architectural possibility (3D-Case #3) which builds upon 3D-Case #2 has been added wherein the z-tows interlace the entire fabric thickness, i.e. instead of interlacing five alternating warp and fill layers, they now interlace nine layers. Figure (7) displays the FE mesh of one layer of 3D-Case #3 which is equivalent to two layers of the first two 3D fabric cases.
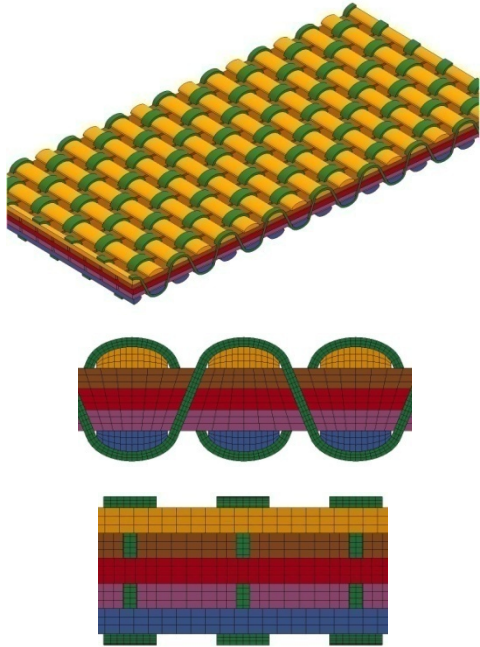
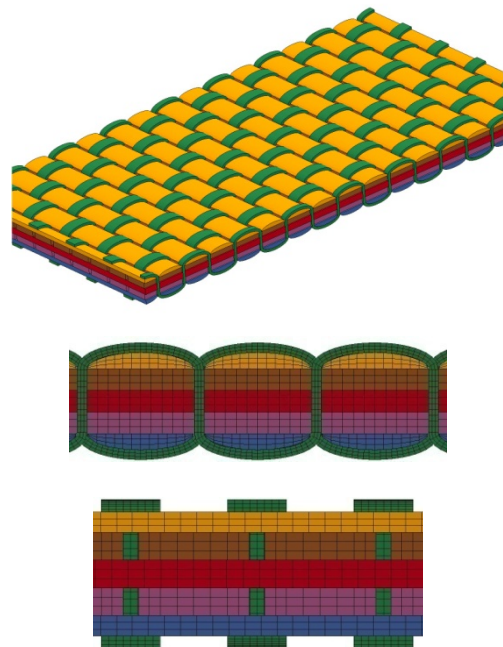*Figure 5. FE model of the one layer of 3D fabric with θ=67.7° (3D-Case #1)*

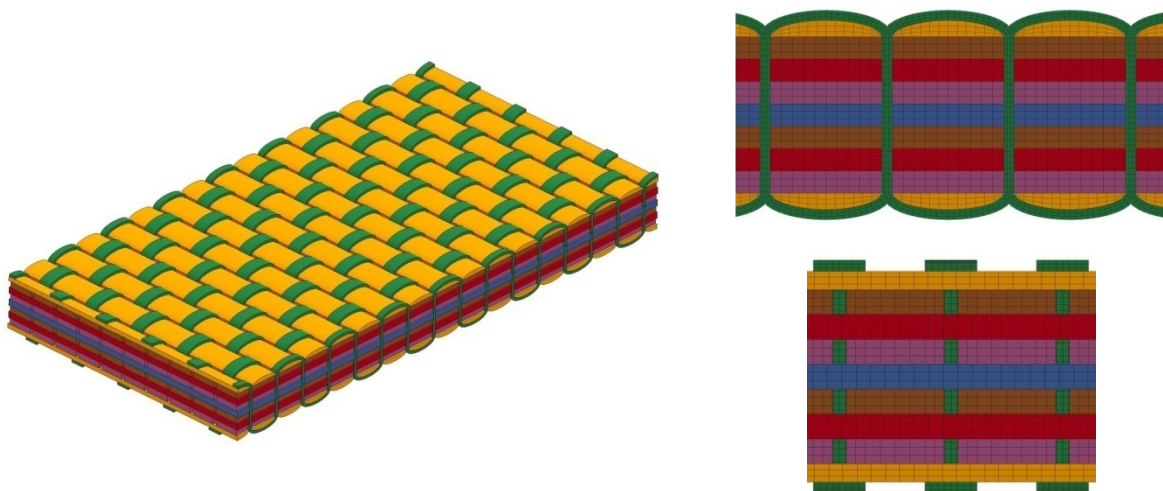*Figure 6. FE model of one layer the 3D fabric with θ=90° (3D-Case #2)*

Figure 7. FE model of one layer of the new 3D fabric with θ=90° (3D-Case #3)

3. SETUP OF THE PROJECTILE FINITE ELEMENT MODELS

To understand the effect of the projectile shape on the impact response for cases of equal intial projectile momentum before impact, two cases are studied. In the first, a rigid cylindrical projectile (Projectile #1) of mass 17.83 gm, diameter 20.8 mm, and height 12.4 mm modeled using shell

elements is used, identical to the projectile in Ref. [1]. Figure (8a) displays the cylindrical projectile. When used with the 2D fabric model, it spans approximately 7 warp yarns, 7 fill yarns, and 8 stitching yarns. When used with the 3D fabric model, it spans approximately 8 warp tows, 7 fill tows, and 9 z-tows. In the second case a rigid spherical projectile (Projectile #2) of similar mass 17.83 gm, and diameter 5.5 mm modeled using shell elements is used. Figure (8b) displays the spherical projectile. When used with the 2D fabric model, it spans approximately 3 warp yarns and 3 fill yarns. When used with the 3D fabric model, it spans approximately 2 warp tows, 3 fill tows, and 3 z-tows. The spherical projectile used here has the same diameter but is heavier than that used in Ref. [1].
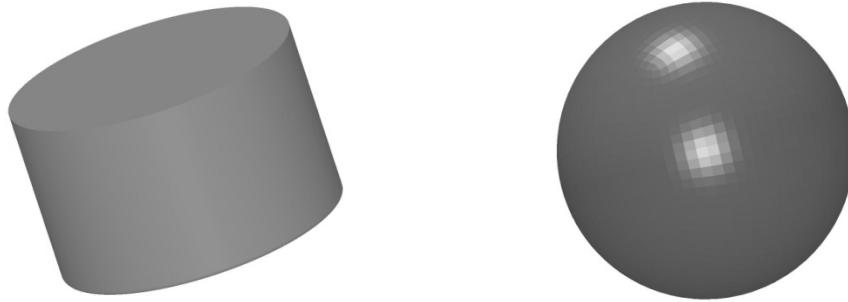
Figure 8. (a) Rigid cylindrical projectile (Projectile #1) (b) Rigid spherical projectile (Projectile #2)

4. COMPARISON OF 2D and 3D FABRIC AND PROJECTILE MASS

Figure (9) compares the total fabric masses of all three models, the mass of the cylindrical projectile, as well as the mass of each fabric component for the studies involving three layers of 2D fabric and one layer of 3D fabric. The mass fraction of the z-tows in 3D fabric case #1 and case #2 are 11.21% and 8.75% respectively. The areal densities of all four fabric models are approximately the same, at 5.115 kg/m^2.
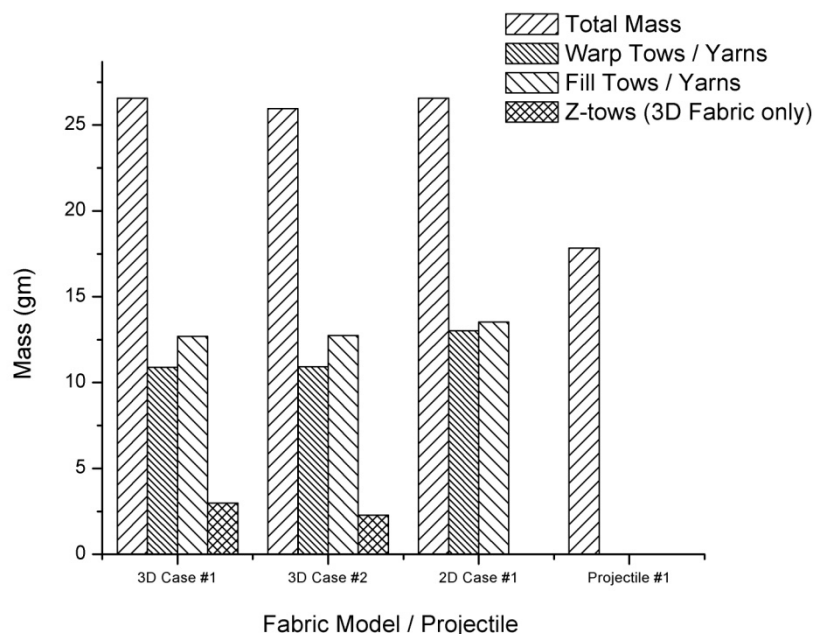
Figure 9. Summary of masses for the equivalent 3-layer 2D fabrics and 1-layer 3D fabrics

Figure (10) compares the corresponding masses for the next part of the study that uses two layers of 3D fabric and an equivalent six layer 2D plain weave fabric. In this study both types of projectiles are

used. The areal densities of all four fabric models are approximately the same, at 10.23 kg/m^2. The mass fraction of the z-tows in 3D-Case #3 is 6.62%.
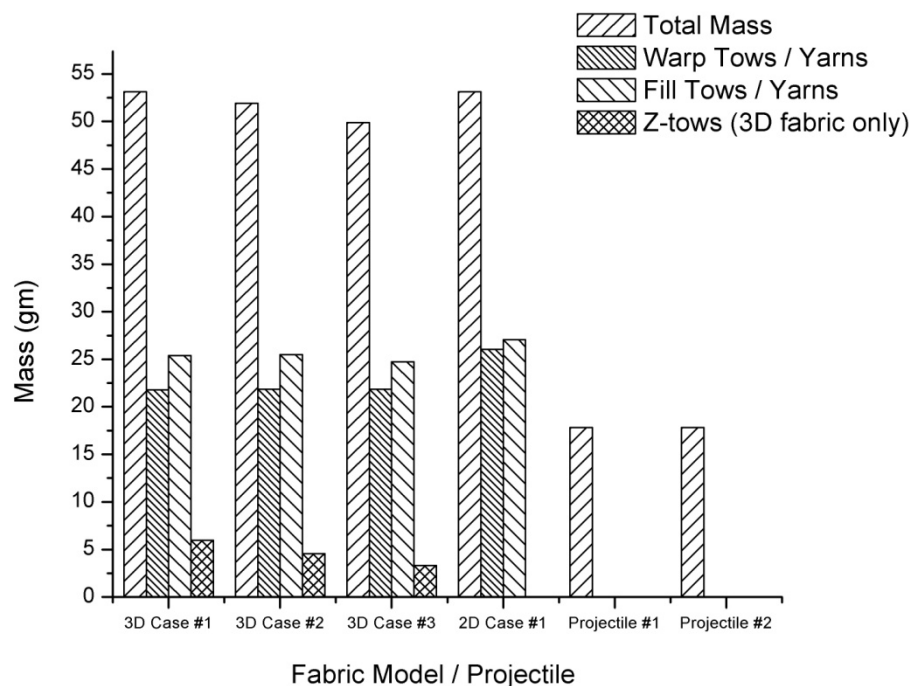

Figure 10. Summary of masses for the equivalent one 6-layer 2D fabrics, two 2-layer 3D fabrics, and one 1-layer 3D fabric

4. RESULTS AND DISCUSSION: EFFECT OF FILL AND Z-TOW MATERIAL PROPERTIES ON IMPACT PERFORMANCE FOR 1-LAYER 3D FABRICS

As an extension of the study in Ref. [1], an impact simulation is set up using LS-DYNA to investigate the effect of z-tow and fill tow material properties on the impact response for the two cases of 3D architecture. The 3D fabric is gripped on all four sides and impacted at the center with a velocity of 60 m/s with the cylindrical projectile. This corresponds to a non-penetrating velocity. A static frictional coefficient of 0.23 is prescribed between the projectile and fabric, and 0.18 between yarns. The material properties for the parametric runs have been modified as followed for the 3D-Case #1: (run A) z-tow made more compliant with E_{11} = 30 GPa from 80 GPa, (run B) fill tow made more compliant and weaker with E_{11}=55 GPa from 80 GPa and σ_{fail} of 2.9 GPa from 3.5 GPa, such that the strain energy density term equal to ($\sigma_{fail}^2/2E_{11}$) remains the same as the fill tow in 3D-Case #1 baseline, (run C) fill tow strength increased with σ_{fail} = 5.0 GPa from 3.5 GPa, and (run D) fill tow made more compliant but retains the same strength with E_{11}=55 GPa from 80 GPa. The material properties for the parametric runs have been modified as followed for the 3D-Case #2: (run A) fill tow strength increased with σ_{fail} = 5.0 GPa from 3.5 GPa.

Figure (11) compares the projectile velocity histories. Details of other simulation results that compare the 3D and 2D architectures can be obtained from Ref. [1]. As earlier stated, 3D-Case#2 outperforms 3D-Case#1as it arrests the projectile earlier and with lesser dynamic deflection. Interestingly, when the fill tow strength was increased to 5 GPa such that no fill tows ever fails, we see that both 3D architectures yield very similar responses, i.e. 3D-Case#1-C and 3D-Case#2-A. Here, the failure of fill tows occurs at the fixed boundaries for those fill tows at the impact location. Also, as seen from 3D-Case#1-A, making the z-tow more compliant has little effect. In other words, the purpose of the z-tow is to keep the warp and fill layers together and needs to be just stiff enough (assuming strength kept

constant) to satisfy this requirement, and any increase in stiffness has little effect since the contribution of the z-tows to overall elastic strain energy is very small. However overly stiff z-tows, assuming the strength is kept constant, may fail prematurely which is severely detrimental to performance. The effect of fill tow compliance with no fill tow failure can be seen from 3D-Case#1-D where a 30% decrease in stiffness results in a small decrease in performance, however on comparing this with 3D-Case#1-B where the fill tow strength was reduced such that impacted fill tows fail, the performance reverts back to the 3D-Case#1 baseline. This set of basic exploratory runs reveal that the strength of fill tows plays a more crucial role than the stifness of the fill tows. The strength and stiffness effects of the warp tows will be investigated later. Further, z-tows only need to be stiff enough to hold the warp and fill layers together, with stiffer z-tows showing no obvious performance benefits for this impact scenario. It is important to keep in mind that when studying z-tows of varying stiffnesses, we are assuming the strength is kept constant. Obviously a z-tow of extremely high stiffness *AND* strength would be ideal. The longer the z-tow is able to keep the layers together before or without failing, the better is the impact performance. Therefore there exist possibilities of patterning the materials used for the z-tows, for example moderate to high strength z-tows of (a) high stiffness, and (b) low stiffness could alternate each other in the 3D fabric such that even if the high stiffness z-tows fail first, the low stiffness z-tows will continue to carry loads and hold the warp and fill tows together, until they too approach the failure strength.
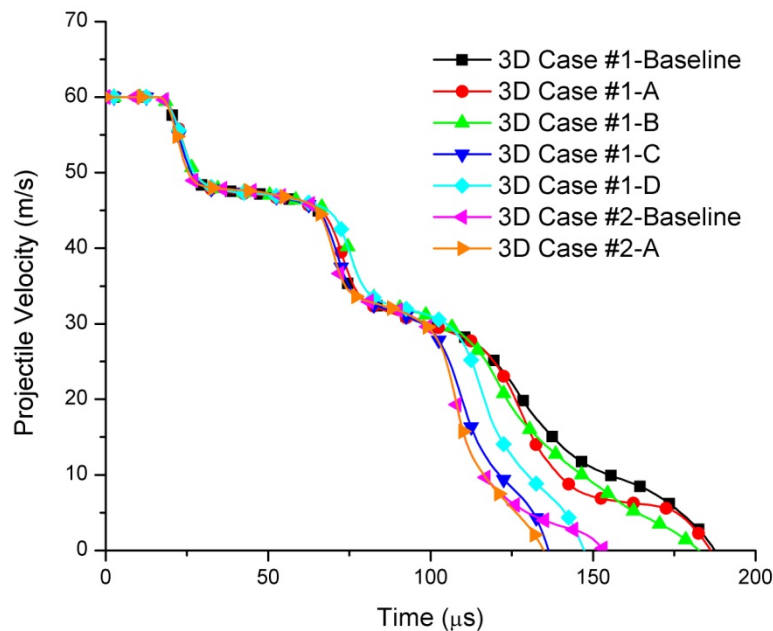

Figure 11. Projectile velocity history for the 3D fabric impact simulations

5. RESULTS AND DISCUSSION: EFFECT OF PROJECTILE SHAPE ON IMPACT RESPONSE OF MULTILAYER FABRIC TARGETS

The cylindrical and spherical projectiles used in this study both have the same mass as seen from Figure (10), however each has a different impact face and spans a different number of yarns are discussed in a previous section. To investigate this effect of the projectile shape in conjunction with the effect of 3D architecture, two impact simulations are set up using both projectiles with an impact velocity of 75 m/s. The fabric is gripped on all four sides. The fabric targets selected consist of two layers of 3D case #1, two layers of 3D case #2, one layer of 3D case #3, and six layers of 2D case #1. All fabric targets have equivalent thicknesses and areal densities as outlined earlier. The fabric material properties remain the same. All reported results account for the quarter symmetric model

implying all extensive results such as fabric internal, kinetic, and frictional energies and momentum have been multiplied by a factor of four, while intensive results such as projectile velocity and projectile-fabric contact force remain unchanged.
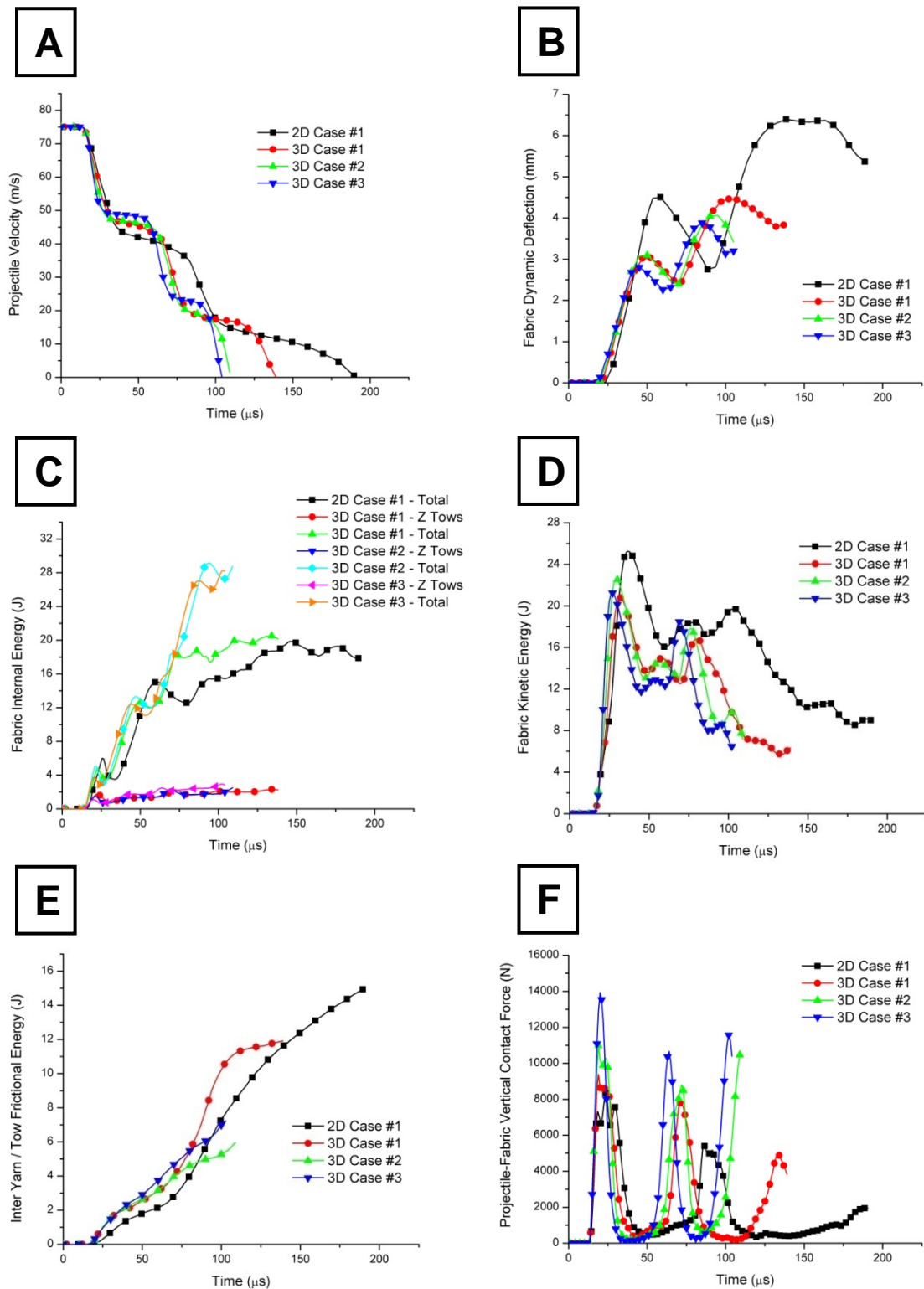

Figure 12. Time history results using the Cylindrical Projectile (a) Projectile velocity (b) Fabric dynamic deflection (c) Fabric internal energy (d) Fabric kinetic energy (e) Inter yarn/tow frictional sliding energy (f) Projectile-fabric contact force

Figure (12) compares the time history results with the cylindrical projectile. All fabric targets are able to completely arrest the projectile without penetration. All 3D fabric cases outperform the 2D fabric case by arresting the projectile earlier and with lower dynamic deflections. Similar to the results reported for single layer impact tests in Ref. [1], these results also show oscillations which indicate separation between the projectile and the fabric layers followed by rebounding of the fabric and reestablishment of contact.
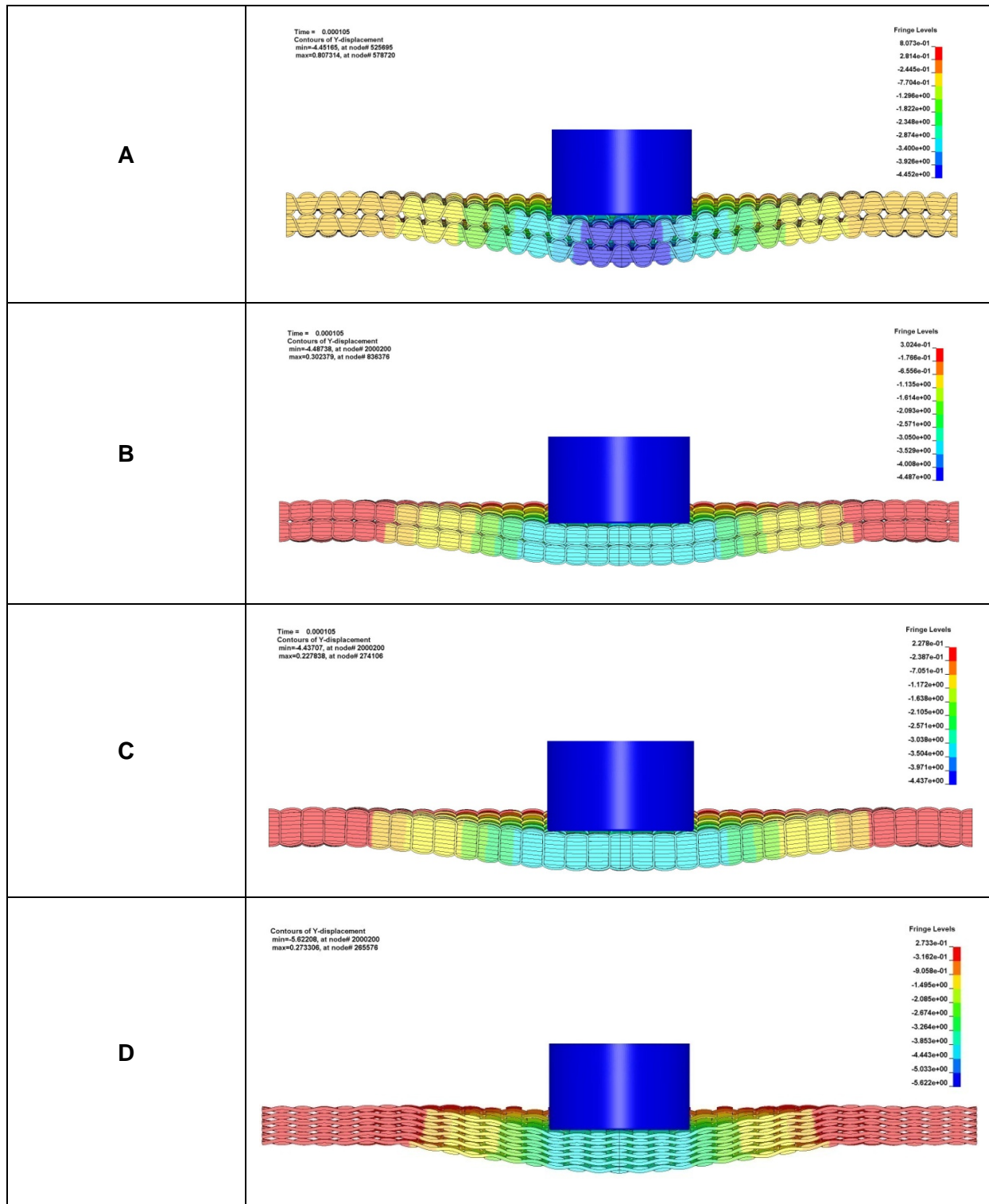
A	
B	
C	
D	

Figure 13. Fabric deformation states using the Cylindrical Projectile at time instant of 105 µs (a) 2 layers of 3D Case #1 (b) 2 layers of 3D Case #2 (c) 1 layer of 3D Case #3 (d) 6 layers of 2D Case #1

The 3D cases with the vertical z-tow inclination arrest the projectile earlier than the case with the inclined z-tows. Figure (13) displays the contours of vertical displacement at the time instant of 105 µs. Interlayer separation is observed for the 2D fabric case only, since there is no through thickness stitching holding the layers together.
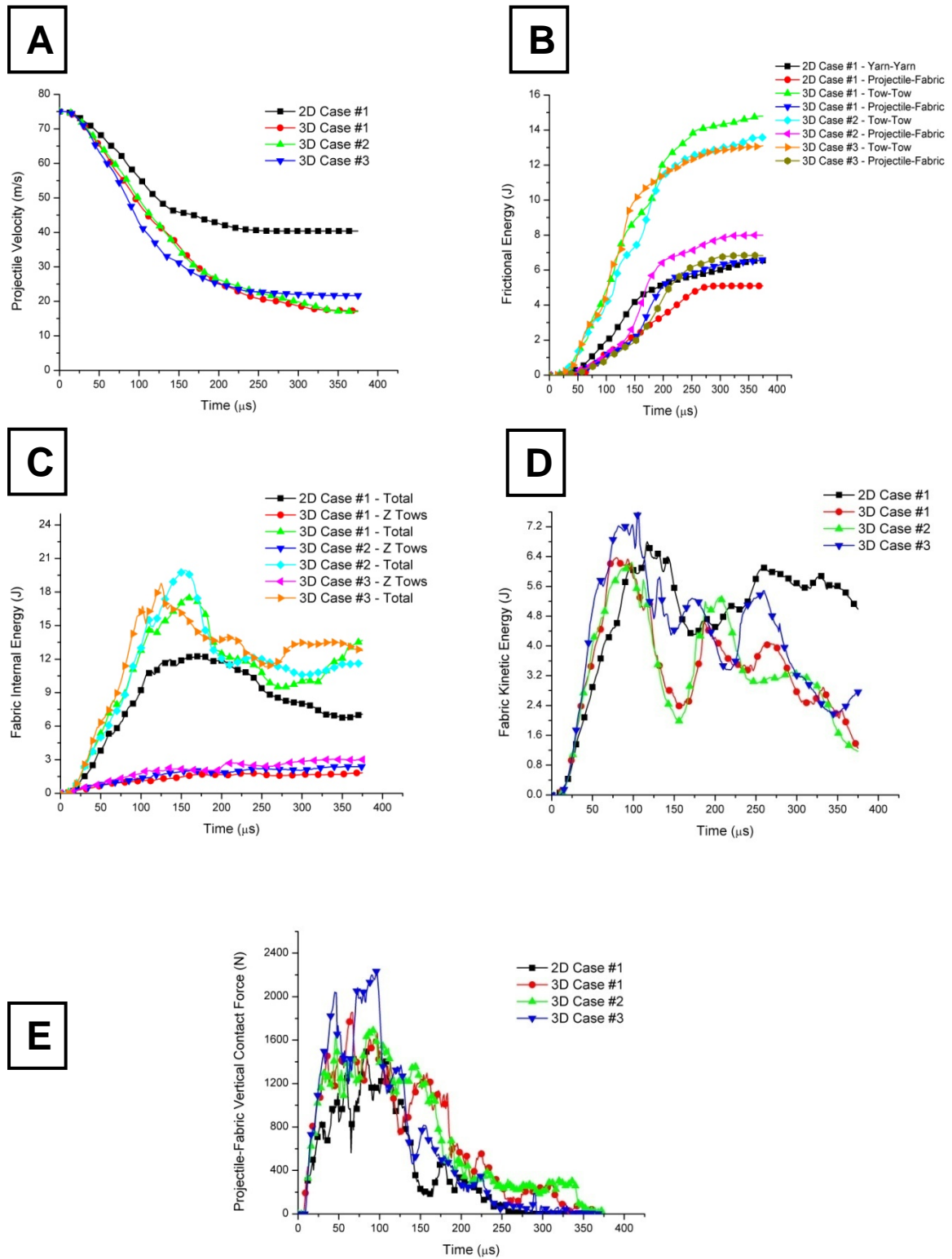

Figure 14. Time history results using the Spherical Projectile (a) Projectile velocity (b) Inter yarn/tow frictional sliding energy (c) Fabric internal energy (d) Fabric kinetic energy (e) Projectile-fabric contact force
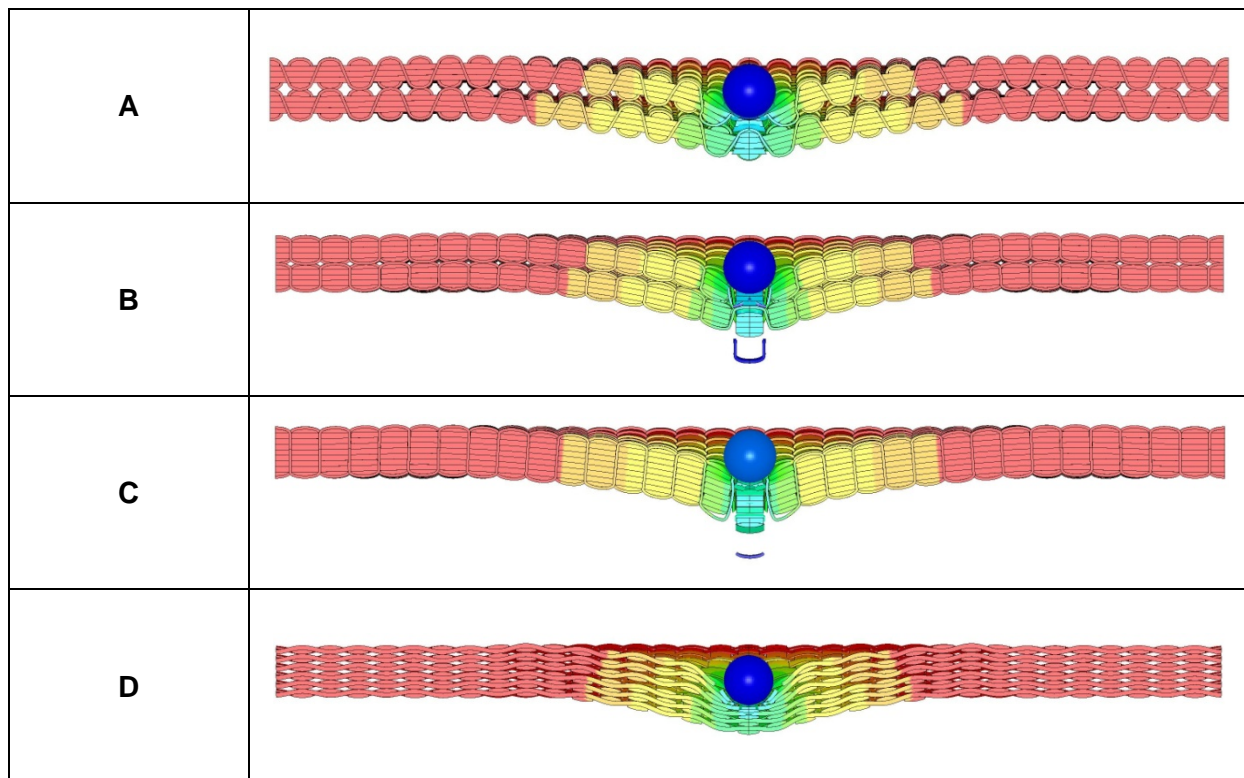
A	
B	
C	
D	

Figure 15. Fabric deformation states using the Spherical Projectile at time instant of 105 µs (a) 2 layers of 3D Case #1 (b) 2 layers of 3D Case #2 (c) 1 layer of 3D Case #3 (d) 6 layers of 2D Case #1

Figure (14) compares the time history results for the spherical projectile impact case. The projectile now penetrates through the fabric for all cases, in spite of having the same initial momentum as the cylindrical projectile. Figure (15) displays the contours of fabric vertical displacement for the time instant of 105 µs. Once again the 2D fabric case is outperformed by the 3D fabric cases. As seen from the results in Ref. [1], the use of stitching yarns greatly improves performance by engaging failed layers that would otherwise separate from the rest of the fabric layers. However as seen from Figure (15), at the time instant of 105 µs, the top layer has been penetrated and no longer contributes to slowing down the projectile as it has been decoupled from the rest of the layers in the absence of stitching yarns. In the absence of a flat impact face, there is no projectile-fabric separation and consequently no oscillations in the time history data. An interesting observation in the projectile velocity history of Figure (14a) is that the 3D case #3 initially decelerates the projectile the fastest. However when the z-tows at the impact zone begin to fail, the fabric structure becomes compromised with little left holding the warp and fill tow layers together, and the projectile velocity history quickly levels off indicating complete fabric penetration. During the time between which the warp and fill tows at the impact site have failed and the projectile has completely penetrated through the fabric, the predominant mechanism by which the projectile velocity is further reduced is frictional sliding between tows due to tow-tow sliding and pullout, and frictional sliding between the projectile and the fabric as the projectile pushes its way through the fabric plies. A gradual decrease in the slope of the velocity history before it completely levels off would indicate a greater level of this frictional sliding. This is observed to a greater extent for the 2D fabric and to a lesser extent in 3D fabric cases #1 and #2, both of which exceed 3D fabric case #3. The magnitude of total frictional energy dissipated by inter-tow sliding in the 3D fabric cases far exceeds that of inter-yarn sliding in the 2D fabric case indicating that surface treatments that increase the coefficient of friction between the tows could have a pronounced beneficial effect since the frictional sliding energy is close in magnitude to the elastic strain or internal energy absorbed by tow elongation. From the projectile velocity history plot in Figure (14a) it is also observed that all 3D fabric cases decelerate the projectile faster than the 2D case. This is due to the absence of tow crimp in the 3D fabrics. However for the 2D fabrics, the warp and fill yarns have to first

decrimp before they can start to elongate in tension thereby slowing down the projectile. This is further inferred from the magnitude of the projectile to fabric contact force which is the highest in 3D-Case #3 as seen in Figure (14e). The vertical component of yarn tension or in-plane membrane tension contributes to the contact force that decelerates the projectile according to the impulse-momentum equation.

6. RESULTS AND DISCUSSION: EFFECT OF IMPACT LOCATION ON 3D FABRIC PERFORMANCE IN THE ABSENCE OF Z-TOWS

It was observed for the spherical projectile impact on 1-layer 3D fabrics during our previous study [1] that the response differed based on the orientation of the z-tow, i.e. whether the z-tow directly underneath the projectile interlaced the fill tow at the top or bottom. The residual projectile velocity was higher when the z-tow was on top and failed soon after being impacted. This was observed only for the spherical projectile case, since its diameter only spanned across a few tows. The response was insensitive when the simulations were repeated using the cylindrical projectile that was much wider and spanned across many tows. To simultaneously investigate the response of a 3D fabric without z-tows i.e. a simple unidirectional composite, and the effect of the impact location on the fabric response, a series of simulations are set up wherein the impact location is set at either directly on the central fill tow that lies on the fabric centerline or in between two fill tows around the fabric centerline, as illustrated in Figure (16). It is expected that as the diameter of the spherical projectile decreases, or as the span of the tows increases, such that the diameter of the projectile approaches the distance between two tows, that the projectile would simply push tows apart at the impact location as it forces its way through the fabric without predominant tow failure by elongation. In such a case, there are no z-tows holding the warp and fill tows together and friction between the projectile and tows that get pushed aside will be the major source of energy dissipation. However the response when the projectile is much larger than the gap between two tows but only spans across a few tows needs to be explored. It is also expected that this effect of impact location be absent for the cylindrical projectile which is much wider and spans across many tows and therefore cannot possibly slide through the gaps in between the tows without tow breakage. Figure (16) displays the FE models of two layers of 3D fabric without z-tows used to study the effect of impact location. In Figure (16a) the projectile directly impacts a fill tow (Configuration #1), while in Figure (16b), the projectile impacts the gap between adjacent fill tows at the fabric symmetry plane or centerline (Configuration #2). Both the cylindrical and spherical projectiles described earlier are used in this part of the study.
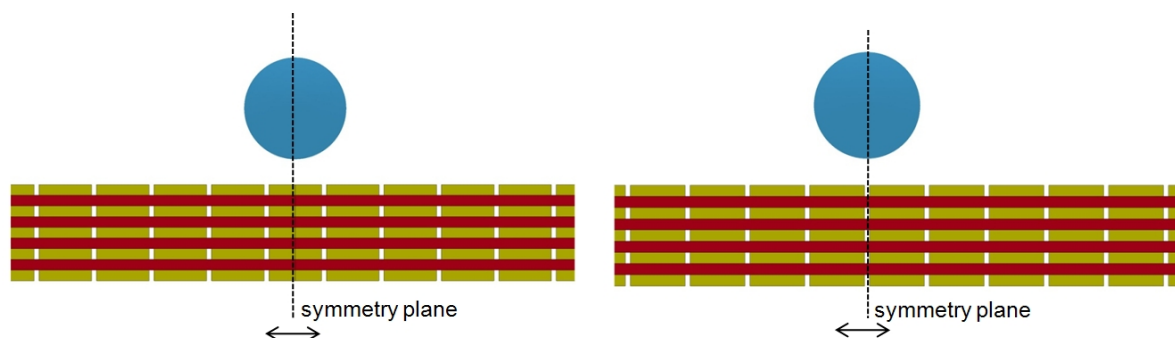

Figure 16. FE models of 3D fabrics without z-tows (left) Configuration #1 (right) Configuration #2

The material properties of the tows and impact test conditions remain the same as outlined earlier in Section 5. Figure (17a) compares the projectile velocity history of the 3D fabric models without the z-tows (*3D No Z Tows - Config #1 and #2*), with the results of the other models, for the spherical projectile impact case at 75 m/s. Surprisingly Config #1 and Config #2 display lower residual velocities than all the other cases. Further, the initial projectile deceleration is similar to that of 3D-Case #3. Figure (18) displays the contours of vertical displacement at the time instant of 105 μs for Config #1. In the absence of z-tows that couple the warp and fill tows, it is seen that all top layer fill tows that were not directly underneath the projectile did not take part in the deformations. Further the two impacted top layer fill tows slide apart from each other as they are pushed aside by the projectile.
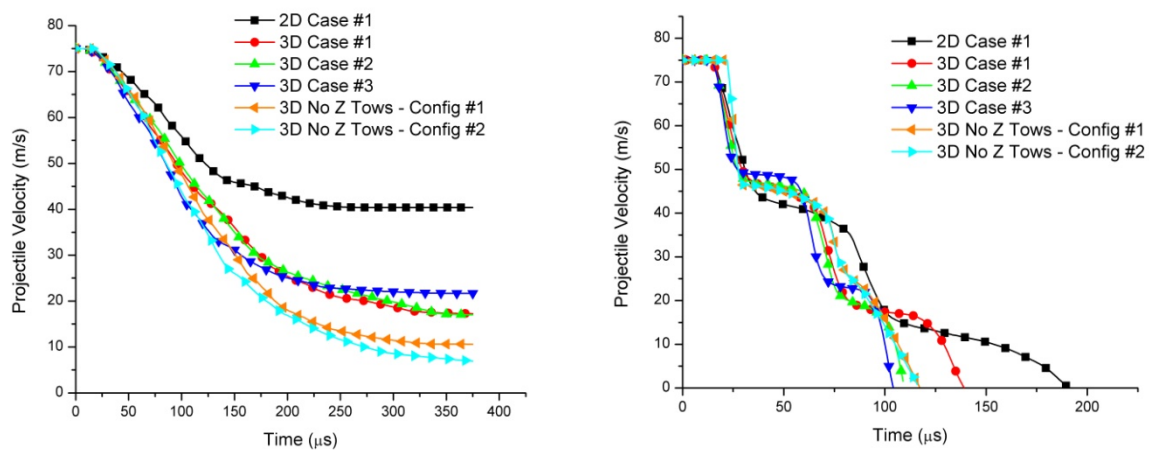
Figure 17. Projectile velocity history for 3D fabric without Z tows Configuration #1 and #2 (left) spherical projectile (right) cylindrical projectile

However because of the very close spacing of the tows, the other tows cannot simply be pushed aside by the projectile and eventually the projectile breaks the warp and fill tows underneath it, as it penetrates through the fabric. Figure (17b) compares the projectile velocity history of the 3D fabric models without the z-tows (*3D No Z Tows - Config #1 and #2*), with the results of the other models, for the cylindrical projectile impact case at 75 m/s. In this case, the performance trend is reversed and Config #1 and Config #2 take slightly longer to arrest the projectile compare to 3D-Case #2 and 3D-Case #3. Also as predicted earlier, both configurations yield almost identical responses indicating that the responses were insensitive to impact location since the diameter of the cylindrical projectile face spanned across many tows.
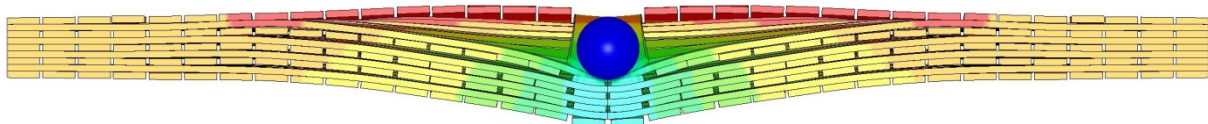

Figure 18. 3D No Z Tows Config #1 fabric deformation states using the Spherical Projectile at time instant of 105 μs

Figure (19) compares the deformation states at the time instant of 120 μs for the cylindrical projectile impact case between 3D-Case #1 and Config #1. Because of the presence of z-tows that couple the warp and fill tows, the deformations and corresponding energy absorptions and momentum transfers are spread out farther in 3D-Case #1. However in Config #1, only those fill tows directly underneath the projectile are deformed. In Figure (19), the tows that have failed are displayed in green, while the tows that remain intact are displayed in red. The presence or absence of z-tows also influences the failure mode. Without z-tows, failure is observed only in the lowest layer with those fill tows separating from the fabric after failing at the boundaries and being ejected. However in 3D-Case #1 which has z-tows, the fill tows fail at the fixed boundaries in all layers however do not separate from the fabric. Also fewer fill tows fail in the Config #1 case. Due to frictional sliding between the failed fill tows in 3D-Case #1, and the interlaced z-tows and warp tows, energy is still being dissipated, however it is not sufficient in magnitude to drastically improve the impact performance. In Ref. [1] we had attributed the improved performance of 3D-Case #2 over 3D-Case #1 to the nature of the z-tow centerline with the former case having a longer path length. Thus the z-tows in 3D_Case #2 exerted less stresses on the interlaced fill tows causing fewer of them to fail. This explanation seems to be confirmed by these results, where now in the absence of z-tows, still fewer fill tows are observed to fail.
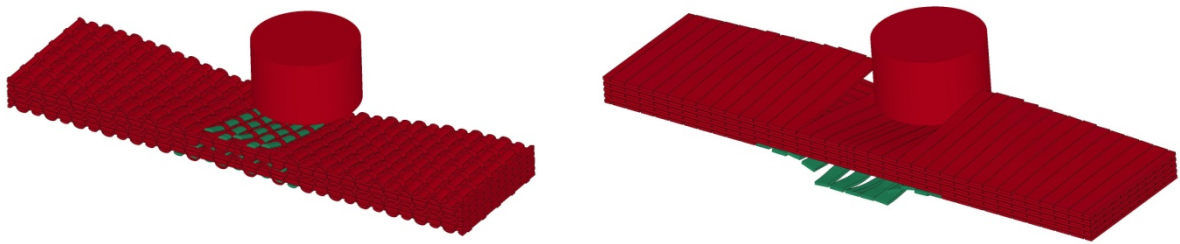
*Figure 19. Failed fill tows at time instant of 120 µs for Cylindrical projectile case
(left) 3D-Case #1 (right) 3D No Z Tows - Config #1*

However a dry 3D fabric without z-tows seems impractical since it lacks structural integrity and cannot be handled easily. Even if it were used when fully impregnated, it would lack interlaminar shear strength compromising its impact performance. By studying the impact response of a 3D fabric without z-tows i.e. a simple unidirectional composite, one preliminary conclusion that emerges is that fabric designs wherein the interlacing tows least interfere with the primary energy absorbers i.e. warp and fill tows yield the best impact response. This is because the z-tows themselves do not absorb much elastic strain energy. Their role is to simply hold the various layers together as well as couple the warp and fill tows to increase the spreading of energy absorption and deformation as far as possible outwards from the impact location.

7. CONCLUSIONS

For the single layer non-penetrating impact tests with the cylindrical projectile, it was seen that increasing the strength of the fill tows at the impact location had a greater benefit than simply increasing their stiffness. Also both 3D fabric Cases #1 and #2 with different z-tow inclinations yielded similar results when the fill tow strength was made large enough such that no fill tow at the impact location fails near the fixed boundaries. However when using fill tows of the same, lower strength, the z-tows with the inclined centerline exerted greater deformations and stresses on the interlaced fill tows causing them to fail earlier, demonstrating that the vertical z-tows with their greater path lengths improved impact performance, as shown in Ref. [1]. Further, increasing the stiffness of the z-tows had little effect, assuming the strength was kept constant. For the double layer impact simulations using projectiles of equal initial momentum, the flat faced cylindrical projectile was completely arrested and started to rebound while the smaller spherical projectile was able to completely penetrate the fabric. The 3D fabrics decelerated the projectile faster than the 2D fabrics due to the absence of two crimp. Further the 3D-Case #3 fabric initially outperformed the other 3D fabric cases until the z-tows at the impact location failed after which it yielded a higher residual velocity. This seems to indicate that having multiple thinner layers (fewer number of warp and fill layers) with interlaced z-tows is more beneficial than having thicker (greater number of warp and fill layers) layers since once the z-tows fail, there is little left holding the warp and fill tows together. However this is not as big a concern with 2D fabrics either with or without through thickness stitching since the warp and fill yarns are woven together.

When comparing 3D fabrics with and without z-tows, an improved performance was observed for the 3D fabrics without z-tows in the penetrating spherical projectile impact case, while a slightly decreased performance was observed for two of the three 3D fabrics in the non-penetrating cylindrical projectile impact case. In the absence of z-tows, all warp and fill tows in the 3D fabric had constant rectangular cross sections and perfectly straight centerlines. The results were sensitive to the impact location, i.e. on the central fill tow or in between two central fill tows, for the spherical projectile which only spanned across a few tows, while it was insensitive for the larger flatter cylindrical projectile. Similarly, the results were sensitive only for the spherical projectile case depending on whether the central z-tow underneath the projectile interlaced the fill tow on top or bottom.

A practical consideration beyond the scope of this study is to consider the tensile strength degradations due to weaving processes. Since the warp and fill tows have no tow crimp in these 3D fabrics, and since they are created through different tow placement processes, their strength

retentions are much higher than corresponding warp and fill yarns in a plain weave fabric, where the fill yarns are impacted into place by a striker bar and there is greater abrasion between the weaving loom and yarns, and between the warp and fill yarns. Abrasion and curvature induced kink bands tend to reduce the tensile strength of yarns and tows. For this reason, the 3D fabrics seem to have an advantage over 2D fabrics. The characterization of the statistical strength distribution and weaving induced damages has been investigated by Nilakantan et al. [2] for Kevlar KM2 yarns from a spool and extracted from Kevlar S706 fabrics, and by Abu-Obaid et al. [3] for S-2 glass fabrics. Nilakantan et al. [4] have presented a methodology to incorporate these statistical distributions of constituent tow material properties into a FE impact simulation. This makes the FE simulation more realistic and predictive in nature and allows for numerical determination of performance parameters such as the V_{50} velocity. However, another consideration is the breathe-ability, and drapability or shearability of fabrics that has a direct correlation with wearer comfort when used as flexible body armor for the torso and extremities, where the fabric needs to adjust to the contours of the human body. Depending on the application and associated constraints, both 2D and 3D fabrics have their own advantages.

The parametric study of material and architectural effects in this study has provided insight into the mechanisms of deformations and interactions that can be used to improve the impact performance of these fabrics, as well as to develop new materials and surface/bulk treatments for the fabrics that could impart improved properties. One example would be a treatment that could increase the coefficient of friction between the tows in the 3D fabric since frictional sliding energy between tows played an important role in overall energy dissipation to slow down the projectile. Future work will continue to investigate the role of materials and architecture in the impact response of 2D and 3D fabrics. As the number of layers increase, it will become important to experimentally characterize the through thickness compression and transverse impact response of these fabrics, which will provide input data to the FE model, as well as provide data to validate the FE models against This will be accomplished through quasi static transverse compression tests using an Instron machine, small and large scale drop impact tests using various span-to-punch ratios, and high rate testing with a compression split Hopkinson bar. Finally the probabilistic simulation approach using experimentally characterized yarn and tow strength data will be implemented as a Monte Carlo approach to assess the impact response, that will complement insight obtained from the parametric deterministic approaches of this study.

ACKNOWLEDGEMENTS

REFERENCES

[1] Gaurav Nilakantan, Michael Keefe, John W. Gillespie Jr., Travis A. Bogetti, Rob Adkinson, "**A Numerical Investigation into the Effects of 3D Architecture on the Impact Response of Flexible Fabrics**", *Second World Conference on 3D Fabrics and their Applications, Greenville, South Carolina, USA*, April 6-7, 2009.

[2] Gaurav Nilakantan, Michael Keefe, John W. Gillespie Jr., Eric D. Wetzel, Travis A. Bogetti, Rob Adkinson, "**An experimental and numerical study of the impact response (V_{50}) of flexible plain weave fabrics: Accounting for statistical distributions of yarn strength**", *The 1st Joint American-Canadian International Conference on Composites and the 24th Annual ASC Technical Conference, University of Delaware, Newark, DE 19711, USA*, September 15-17, 2009.

[3] Ahmad Abu-Obaid, Steve M. Andersen, John W. Gillespie, Jr., B. Dickenson, A. Watson, G. Chapman, R. A. Coffelt, "**Effects of weaving on S-2 glass tensile strength distributions**", *TEXCOMP 9, University of Delaware, Newark, DE, USA*, October 13-15, 2008.

[4] Gaurav Nilakantan, Michael Keefe, John W. Gillespie Jr., Travis A. Bogetti, "**Modeling the material and failure response of continuous filament fabrics for use in impact applications**", *TEXCOMP 9, University of Delaware, Newark, DE, USA*, October 13-15, 2008.